JOURNAL OF MAGNETIC RESONANCE 88, 9–19 (1990)

Transverse Relaxation Processes in Porous Sedimentary Rock

R. L. KLEINBERG AND M. A. HORSFIELD*

Schlumberger-Doll Research, Old Quarry Road, Ridgefield, Connecticut 06877-4108

Received September 18, 1989

Transverse relaxation rates of a number of water-filled porous rock samples have been measured as a function of static magnetic field strength and Carr–Purcell pulse spacing. At the lowest field and shortest pulse spacings, T_2 appears to be dominated by relaxation at the fluid–solid interface, while at higher fields and longer pulse spacings, there is clear evidence of molecular diffusion in a magnetic field gradient. This gradient is due to the magnetic susceptibility contrast between grain material and the pore fluid. Samples with small pores show the strongest evidence for restriction of diffusion, and a broad distribution of pore sizes is another important complicating factor. A theory which takes into account all the above effects in a consistent manner has been developed; the total relaxation rate is not simply the sum of the relaxation rates of the individual processes. With parameter selection guided by independent measurements of magnetic susceptibility and pore size, the theory adequately reproduces experimental results.

Nuclear magnetic relaxation processes of fluids in restricting geometries are of interest in a wide variety of materials and systems. Fluids contained in biological cells, porous inorganic compounds such as zeolites, and packings of regular and irregular particles have all been the subject of NMR investigations. Molecular diffusion in these media has been of particular interest; a recent review (*1*) contains a summary of the field. Water-saturated sedimentary rocks constitute an unusually complex system in which to study restricted diffusion: the pore space is usually heterogeneous in both size and shape. Also, the surfaces of the solid grains play an active part in relaxation of the pore fluid, but are not the sole source of relaxation. Furthermore, internal magnetic field gradients vary considerably from point to point within the pore space.

Nevertheless, there has been considerable interest in the study of the NMR relaxation behavior of water-saturated rock samples (*2–4*). There is potential for NMR techniques to yield valuable petrophysical information from oil well-bore logs: the total fluid content and the permeability of the formation are of fundamental importance to oil recovery efficiency. Furthermore, NMR imaging and spectroscopy techniques may be used for detailed analysis of rock cores brought to the surface (*5*).

Usually, longitudinal relaxation rates are used to estimate the petrophysical properties of the rock (*6*), but the transverse relaxation rates can give equally valuable information. When using a spin-echo sequence, it is well known, however, that the rate of

* Present address: Herchel Smith Laboratory for Medicinal Chemistry, University of Cambridge School of Clinical Medicine, University Forvie Site, Robinson Way, Cambridge CB2 2PZ, United Kingdom.

0022-2364/90 $3.00

decay of transverse magnetization is strongly affected by the presence of diffusion through magnetic field gradients. The molecular motion causes a random variation of the Larmor frequency of a given nucleus, resulting in a more rapid loss of coherence than would be expected from consideration of the usual spin–spin interactions alone. The resulting echo attenuation can be reduced by employing the multiple-pulse (CPMG) technique of Carr and Purcell (*7*) as modified by Meiboom and Gill (*8*), but the high internal gradients present in heterogeneous systems can make it difficult to eliminate the attenuation effectively. Alternatively, this effect may be exploited, and many studies have been made of the effect of an externally applied one-dimensional linear field gradient on transverse relaxation behavior (*9*), this technique being used to measure diffusion coefficients and also, in the case of restricted diffusion, to estimate the dimensions of the restricting boundaries (*10*).

In porous media, the internal magnetic field gradients are caused by the different susceptibility values of the solid grains and the pore fluid, the form of the gradient depending on the geometry of the pore structure and the magnitude being directly proportional to the applied magnetic field strength. For rocks, the situation is further complicated because the diffusion is restricted in the pore space (*11*). If, however, the pulse spacing in the CPMG sequence can be made short enough, or the internal field gradient strengths can be reduced by a reduction of the applied magnetic field, then transverse relaxation is dominated by contact between the relaxing spins and the surface of the rock matrix.

For the present study, the relaxation properties of a suite of six sandstones and two carbonates were measured. The samples span a broad range of porosities and pore sizes. The range of echo spacings and static field strengths used allowed exploration of both grain-surface-dominated and diffusion-dominated relaxation regimes. A theory is presented which accounts for the effects of bulk relaxation, surface relaxation, the internal magnetic field gradients, and restricted diffusion. When these factors are combined in a consistent manner which explicitly takes into account the distribution of pore sizes, the total relaxation rate is not simply the sum of the relaxation rates of the individual processes.

EXPERIMENTAL METHODS

All NMR measurements were performed using a Bruker CXP spectrometer equipped with an electromagnet capable of giving proton Larmor frequencies up to 90 MHz. The cores used were 8 mm in diameter and 10 mm long. Sample temperature was regulated to 313 K, and the cores were held in 10 mm NMR tubes under fluorinated oil to prevent water evaporation during the course of the experiment. The CPMG sequence was used for transverse relaxation measurements

$$90^\circ_{(x,-x)}—t_{cp}—[180^\circ_{(y)} - 2t_{cp}]_n$$

with t_{cp} varying from 45 μs to 1.8 ms. The subscripts denote the phases of the pulses in the phase-cycling scheme used to remove any baseline offsets. A single data point was acquired at the center of each echo, with up to 2048 data points being collected. Phase-sensitive detection was used for all measurements, the receiver phase being adjusted to give maximum signal amplitude in the in-phase channel.

Normally, porous media exhibit a spread of relaxation rates which reflects the distribution of pore sizes present. The transverse relaxation data were therefore analyzed using the stretched-exponential model of Kenyon *et al.* (*6*):

$$M(2nt_{cp}) = M_0 \exp\left(\frac{-2nt_{cp}}{T_2}\right)^{\alpha}. \quad [1]$$

This allows for a distribution of relaxation rates while keeping the number of variable fit parameters small.

Measurements were made at three field strengths corresponding to proton Larmor frequencies 5, 40, and 90 MHz, but because of the greater RF power requirements at high operating frequencies, the transverse relaxation rates could only be measured with the longer t_{cp} values at the two higher field strengths.

THEORY

The results of transverse relaxation measurements made on two of the rocks, Berea sandstone and Leuders limestone, are shown in Figs. 1a and 1b. The eight rocks showed a range of behavior, of which these two examples are representative. The transverse relaxation rate is plotted against $B_0^2 t_{cp}^2$, which anticipates the importance of diffusion at long values of t_{cp} and at high values of magnetic field strength (*7*). At the lowest values of $B_0^2 t_{cp}^2$ the transverse relaxation rates are independent of t_{cp}. The values of $1/T_2$ in the limit $B_0 t_{cp} \rightarrow 0$ are well in excess of the relaxation rate for pure water under the same conditions, which was measured as 0.3 s^{-1}. This indicates that significant relaxation is occurring due to the presence of the grain surfaces.

At higher values of $B_0^2 t_{cp}^2$, there is clear evidence of the effect of molecular diffusion in the presence of a static magnetic field gradient. The Carr–Purcell equation (*7*) for the measured value of T_2 is

$$\frac{1}{T_2} = \frac{1}{T_{2o}} + \frac{D}{3}(\gamma G t_{cp})^2, \quad [2]$$

where $(1/T_{2o})$ is the relaxation rate due to all other processes, γ is the gyromagnetic ratio of the resonant nucleus, G is the static magnetic field gradient, and D is the diffusion coefficient of the liquid. The mean magnetic field gradient caused by the inhomogeneity of the magnet used to collect the data was measured to be better than 2.0 mT m^{-1} at a field strength of 1.0 T. This is far too small to account for the pulse-spacing-dependent relaxation rate, so we presume that magnetic field gradients within the porous sample itself (*12*) are responsible for the enhanced relaxation rate.

It can be seen that although Eq. [2] can be employed usefully to explain the behavior of Berea sandstone, it clearly fails to describe the Leuders limestome results. From the mercury porosimetry measurements, we know that the median pore size of the Berea sample is more than 30 times that of the Leuders sample. Therefore, we conclude that Eq. [2] is inadequate when the diffusion of molecules in porous solids is restricted by the presence of impenetrable boundaries. This complicating factor has been considered in previous work (*13–16*). It is our purpose to extend this work to encompass the effect of a distribution of pore sizes, and in doing so we shall find it

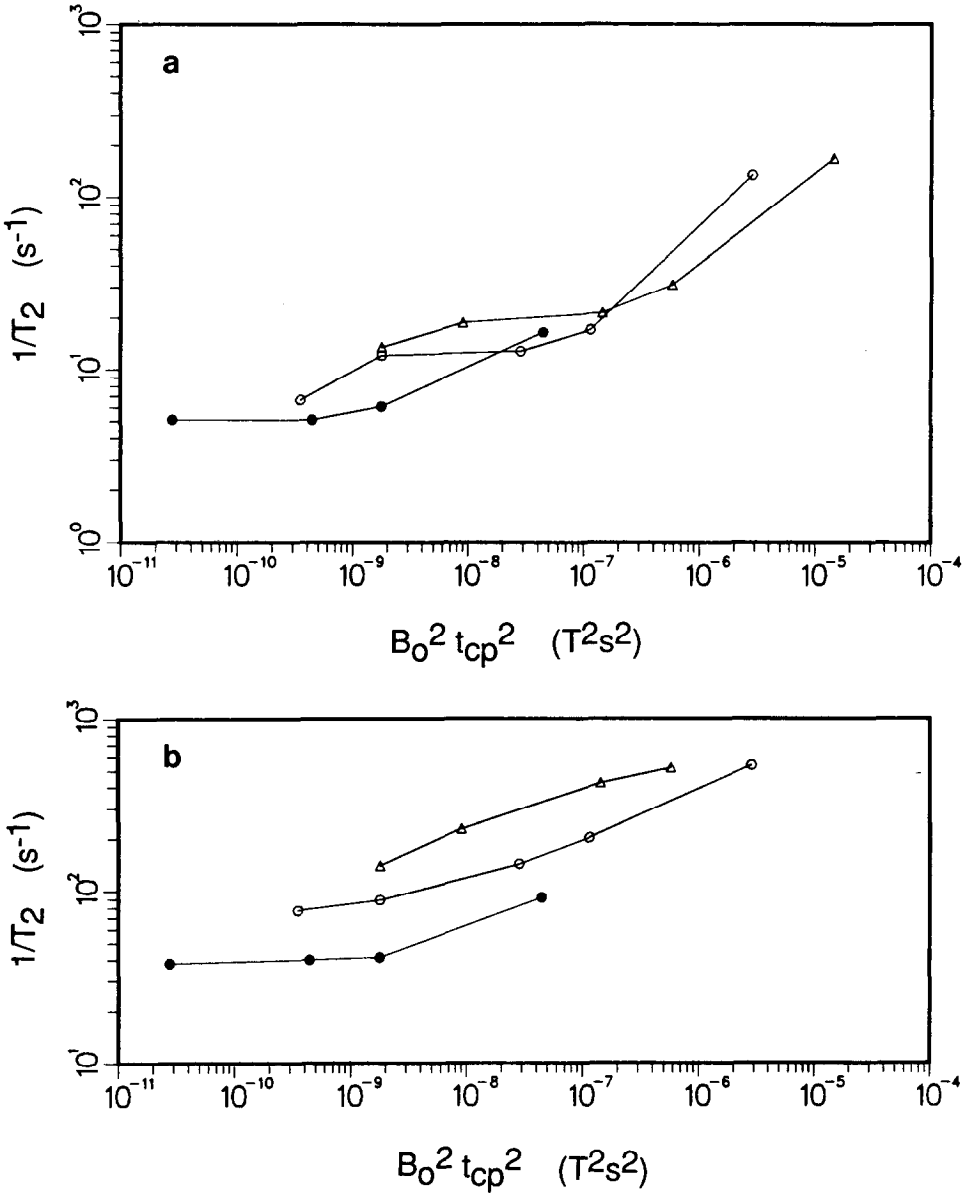

FIG. 1. The variation of the transverse relaxation rate of (a) Berea sandstone and (b) Leuders limestone with the static field strength and the Carr–Purcell pulse spacing. Experimental data points are shown for three proton resonance frequencies: 5 MHz (solid circles); 40 MHz (open circles); 90 MHz (open triangles).

necessary to develop a model which treats grain-surface relaxation simultaneously with diffusion-related relaxation.

Magnetic relaxation due to diffusion in a single pore. Neuman (*15*) derived equations describing the decay of transverse magnetization due to restricted molecu-

TABLE 1

Roots of $\tan(\alpha_i) = 2\alpha_i/(2 - \alpha_i^2)$

i	α_i
1	2.081576
2	5.940370
3	9.205839
4	12.40444
5	15.57923
6	18.74265
7	21.88279

lar diffusion in a uniform field gradient. Three geometries were considered: planar, spherical, and cylindrical; the three equations have the same general form. Microscopic examination of rock samples shows the pores to be irregularly shaped. However, they are closer to spherical than to planar or cylindrical, so we use

$$M(t) = M_0 \exp\left[-\frac{2\gamma^2 G^2 R^4 t}{D} \sum_{i=1}^{\infty} \left(\frac{1}{\alpha_i^4(\alpha_i^2 - 2)} \right) \times \left(1 - \frac{3 - 4\exp(-a/2) + \exp(-a)}{a} \right) \right], \qquad a = \frac{\alpha_i^2 Dt}{R^2}, \quad [3]$$

where R is the pore radius. The numerical coefficients α_i ($\alpha_m R$ in Neuman's notation) are the solutions of the transcendental equation

$$\alpha_i J'_{3/2}(\alpha_i) - \tfrac{1}{2} J_{3/2}(\alpha_i) = 0. \quad [4]$$

$J_{3/2}(x)$ is the Bessel function of order 3/2, and $J'_{3/2}$ is its derivative with respect to its argument. Using the identities of spherical Bessel functions (*17*), it may be shown that Eq. [4] reduces to

$$\tan(\alpha_i) = \frac{2\alpha_i}{(2 - \alpha_i^2)}. \quad [5]$$

The first seven nonzero roots are given in Table 1. Asymptotically, the roots are given by $\alpha_i = i\pi$.

The Neuman equation must be modified when a Carr–Purcell (CP) pulse sequence is used. For any magnetization decay which can be described by

$$M(t) = \exp(f(t)) \quad [6]$$

it is easy to show that the magnetization of the nth echo of a CP sequence is

$$M(2nt_{cp}) = \exp(nf(2t_{cp})). \quad [7]$$

Therefore, the transverse magnetization decay in a CP sequence can be described by

$$M(t) = M_0 \exp\left[-\frac{2\gamma^2 G^2 R^4 t}{D} \sum_{i=1}^{\infty} \left(\frac{1}{\alpha_i^4(\alpha_i^2 - 2)} \right) \times \left(1 - \frac{3 - 4\exp(-a/2) + \exp(-a)}{a} \right) \right], \qquad a = \frac{2t_{cp}\alpha_i^2 D}{R^2}, \quad [8]$$

where $M(t)$ is measured at the center of the echoes.

Internal magnetic field gradients. At the outset, we encounter a serious problem in characterizing the static magnetic field gradient. This gradient arises from the magnetic susceptibility contrast between pore fluid and solid grains. One might start by approximating a pore as an ellipsoid of revolution, for which the magnetic fields may be calculated analytically. Standard textbooks (*18*) treat the electric field case, which is perfectly equivalent to the magnetic field case. If a uniform field is applied to an ellipsoid, the resulting internal field is uniform and parallel to the applied field, regardless of the orientation of the ellipsoid axes. Therefore the gradients must arise because the pore space is irregularly shaped, which microscopic examination manifestly demonstrates is the case.

Glasel and Lee (*19*) have calculated the field gradient outside a single sphere (representing a grain) having a magnetic susceptibility differing from that of an external medium (representing the fluid-filled pore space). For a region close to the sphere the average gradient is

$$G = \mu_0 H_0 \Delta\chi / 4R_g, \quad [9]$$

where μ_0 is the magnetic permeability of vacuum, H_0 is the applied magnetic field strength, $\Delta\chi$ is the difference between the volume magnetic susceptibilities of the sphere and the external medium, and R_g is the radius of the sphere. Because the grains themselves are irregularly shaped, we interpret R_g as a local radius of convex curvature. We further assume that the local radius of curvature is roughly the same as the radius of the pore itself. We are not satisfied by these approximations, but in the absence of a detailed stereological study of the pore space, we are not sure how to better characterize the magnitude of the field gradient within individual pores.

A more sophisticated approach has been taken by Majumdar and Gore (*20*): they sum the fields due to an array of spheres immersed in the medium. This model works well for a dilute system of spheres, but its validity is questionable when the grains themselves are highly irregular and densely packed. Therefore the benefits derived from using this detailed model do not warrant the attendant computational complexity.

Other transverse magnetic relaxation mechanisms. Brownstein and Tarr (*21*) analyzed the manner in which magnetization of fluids decays in a cell of characteristic dimension R. An essential element of their model is a bounding surface which has a certain probability of relaxing spins that come in contact with it. This surface is characterized by the parameter ρ (Brownstein and Tarr use the symbol M) which intuitively may be thought of as the thickness of the fluid layer that may be influenced by the surface, divided by the surface relaxation time. Contained in the cell is a fluid having diffusion coefficient D. When the surface is efficient at relaxing the spins, that

is, when $\rho R/D \gg 1$, the relaxation rate is controlled by the time it takes for molecules to diffuse to the surface, and, approximately,

$$M_s(t) = M_0 \exp(-Dt/R^2). \quad [10]$$

when the surface is an inefficient relaxation agent, $\rho R/D \ll 1$, the magnetization is described by

$$M_s(t) = M_0 \exp(-\rho t(S/V)), \quad [11]$$

where (S/V) is the surface to volume ratio of the pore; in the approximation that the pore is spherical, $S/V = 3/R$.

The parameter ρ can be different for longitudinal and transverse relaxation, giving rise to different relaxation parameters ρ_1 and ρ_2. On the basis of a study of many rocks, Kenyon *et al.* (*6*) have concluded that Eq. [11] is applicable for T_1 processes. We assume that the same is true for T_2 processes.

Acting in parallel with the wall relaxation mechanism is the normal bulk liquid relaxation process, with transverse relaxation time T_{2b}. If the pore fluid is water, this contribution is normally insignificant. When the pore fluid is a viscous oil (*22*), or a solution with a high density of paramagnetic ions, bulk relaxation mechanisms may dominate.

Pore size distribution. A number of groups have used NMR relaxation data to determine the pore size distribution of rocks. Kenyon *et al.* (*6*) pointed out that the observed stretched exponential decay of longitudinal magnetization can arise from a population of pores of various sizes, the spins in each pore relaxing according to Eq. [11]. In an obvious extension to the work of Kenyon *et al.*, we may write

$$\exp\left(-\left(\frac{t}{T_1}\right)^{\alpha}\right) \approx \int_0^{\infty} dR \exp\left(-\left(\frac{R}{R_0}\right)^{\alpha/(1-\alpha)}\right)\exp\left(-\left(\frac{3\rho_1}{R}t\right)\right). \quad [12]$$

Measurements on more than 100 water-filled rocks showed that α is generally around 2/3. Therefore, the pore size distribution can be presumed to be Gaussian,

$$P(R) = \exp\left(-\left(\frac{R}{R_0}\right)^2\right), \quad [13]$$

where R_0 is a characteristic length scale. $P(R)$ is the volumetric probability density; i.e., it is the volume of the population of pores having radius R. Thus the total pore volume is given by

$$V = c\int_0^{\infty} dR \exp\left(-\left(\frac{R}{R_0}\right)^2\right), \quad [14]$$

where c is a constant having dimensions of length squared.

Unified equation for transverse relaxation. We can now describe transverse relaxation in a rock having a distribution of pore sizes and associated distribution of surface and diffusion-related relaxation rates. When a relaxation mechanism operates in parallel with and is independent of other relaxation processes, as is the case with bulk relaxation, then the relaxation rates are additive. Robertson (*14*) showed that

diffusion-related and surface relaxation are also independent to second order so that, within a single pore, the resulting relaxation rates may be added.

However, the decay processes are functions of the pore size, giving rise to a decay of transverse magnetization which will be nonexponential. Hence it is necessary to calculate $M(t)$ explicitly as the sum of magnetization from the distribution of pores and find T_2 from the resulting decay curve.

With these points in mind, we combine Eqs. [8], [9], [11], and [13] to find

$$M(t) = M_0 \int_0^\infty dR \exp\left(-\left(\frac{R}{R_0}\right)^2\right)\exp\left(-\frac{3\rho_2}{R}t\right)\exp\left(-\frac{1}{T_{2b}}t\right)\exp\left[-\frac{2\gamma^2 G^2 R^4 t}{D}\right.$$

$$\left.\times \sum_{i=1}^{\infty}\left(\frac{1}{\alpha_i^4(\alpha_i^2-2)}\right)\left(1-\frac{3-4\exp(-a/2)+\exp(-a)}{a}\right)\right], \quad a=\frac{2t_{cp}\alpha_i^2 D}{R^2}. \quad [15]$$

The complexity of the argument of the fourth exponential function of this equation makes analytical solution difficult. The equation was therefore solved numerically, the integral being evaluated using an adaptive Romberg extrapolation algorithm as embodied in a commercially available computer subroutine (*23*). The sum usually converges to one part in 10^4 in a few terms. T_2 was determined from Eq. [15] by the condition $M(T_2) = M_0/e$, which is consistent with Eq. [1].

We will compare the predictions of Eq. [15] with a formulation that accounts for the effect of a distribution of pore sizes on the surface relaxation rate and magnetic field gradient, but allows for unrestricted diffusion. The appropriate equation is

$$M(t) = M_0 \int_0^\infty dR \exp\left(-\left(\frac{R}{R_0}\right)^2\right)\exp\left(-\frac{3\rho_2}{R}t\right)\exp\left(-\frac{1}{T_{2b}}t\right)\exp\left(-\frac{Dt}{3}(\gamma G t_{cp})^2\right). \quad [16]$$

Selection of parameters. The transverse relaxation rate of Leuders limestone, measured as a function of B_0 and t_{cp}, showed the largest departure from the predictions of the Carr–Purcell theory, Eq. [2]. Therefore, it provides the best example of the applicability of the new theory, Eq. [15]. The material constants which enter into Eq. [15] are the characteristic pore size, R_0; the magnetic susceptibility contrast between the grains and the pore fluid, $\Delta\chi$; the surface relaxation parameter, ρ_2; the diffusion constant of the pore fluid, D; and the fluid bulk relaxation time, T_{2b}. We have either independently measured or used published values for all of these except ρ_2, which is difficult to determine separately.

The pore size distribution of the Leuders limestone was measured by mercury injection porosimetry (Micromeritics Autopore II porosimeter) which gives an indication of the size of restricting throat associated with the pore into which the mercury intrudes. Thus, the radius measured bears only an approximate relationship to the pore radius, the correspondence depending on the exact pore geometry. The pressure at which mercury had intruded into one-half of the total pore volume was 1.62 MPa (235 psi). Using the standard equations of mercury porosimetry (*24*), this implies a median pore radius, R_v, of 0.45 μm.

The relationship between R_v and R_0 of a Gaussian distribution is expressed by

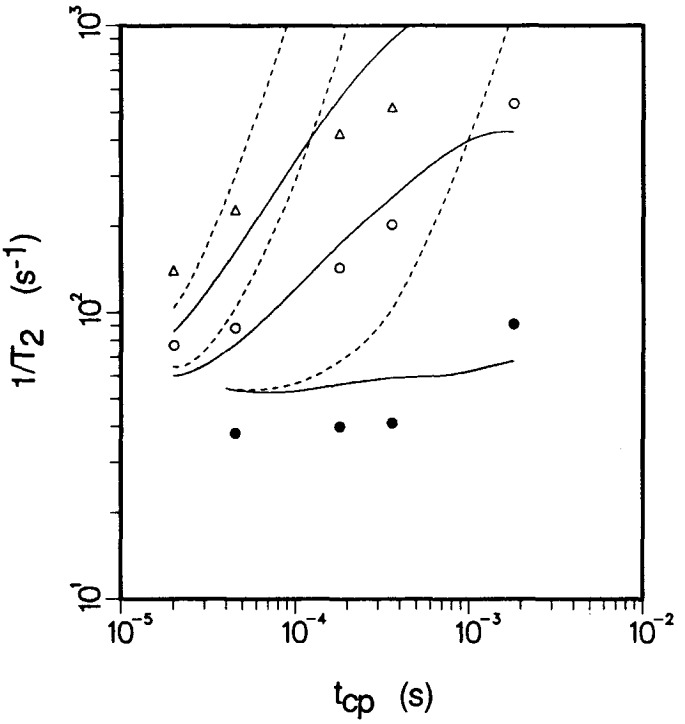

FIG. 2. Transverse relaxation rate of Leuders limestone as a function of the time between the 90° pulse and the first 180° pulse in a Carr–Purcell pulse train. Symbols as in Fig. 1. The three solid curves are the restricted diffusion theory for the same three frequencies. The parameters used were $R_0 = 2\ \mu m$, $\Delta\chi = 75 \times 10^{-6}$, and $\rho_2 = 1.6 \times 10^{-6}\ m\ s^{-1}$. The three dashed curves are the predictions of the unrestricted diffusion theory, using the same parameter set.

$$\frac{1}{2} = \frac{\int_0^{R_v} dR \exp(-(R/R_0)^2)}{\int_0^{\infty} dR \exp(-(R/R_0)^2)} \qquad [17]$$

with the result that $R_0 = R_v/0.475$. Hence the mercury porosimetry measurement gives $R_0 = 0.96\ \mu m$.

The measured relaxation time of the water used to saturate the rocks was $T_{2b} = 3$ s at 40°C. The diffusion coefficient of water at 40°C, measured by NMR techniques (*25*), is $D = 3.14 \times 10^{-9}\ m^2\ s^{-1}$.

The magnetic susceptibility required for Eq. [9] is the volume magnetic susceptibility, χ_v, defined by

$$B = \mu_0 H_0 (1 + \chi_v). \qquad [18]$$

Its value for water is -9.26×10^{-6} in S.I. units. Many rocks have significant content of paramagnetic ions which dominate their magnetic properties. The grain mass susceptibility of Leuders limestone was measured using a Gouy balance to be $3.0 \times 10^{-9}\ m^3\ kg^{-1}$. The grain density is $2.71 \times 10^3\ kg\ m^{-3}$, so the volume susceptibility is 8.1×10^{-6}. $\Delta\chi$ is then 17×10^{-6}.

To our knowledge there are no published data on the grain-surface transverse relaxation parameter, ρ_2, in rocks. Moreover, the microscopic mechanism controlling ρ_2 is unknown. We assume that ρ_2 is independent of Larmor frequency, and its value is allowed to be a variable parameter.

RESULTS

Equation [15] was used to calculate transverse relaxation rates as a function of Carr–Purcell pulse spacing for proton resonance frequencies of 5, 40, and 90 MHz. The results are shown as solid curves in Fig. 2. At the lowest values of t_{cp} and static field strength, $1/T_2$ is dominated by grain-surface relaxation, as expected. At higher values of t_{cp} and field, the effects of diffusion in a field gradient become apparent. However, these effects saturate at the largest values of t_{cp}. Clearly, this indicates the inability of the spins to experience arbitrarily large changes in their precession frequency between the 180° pulses in the Carr–Purcell sequence.

The experimentally determined transverse relaxation rates of Leuders limestone for the same three frequencies are shown as points in Fig. 2. The restricted diffusion theory generally follows the experimental data points. The exception is at the longest value of t_{cp} (1.8 ms), where the theory underestimates $1/T_2$. The effect of unrestricted diffusion, calculated using Eq. [16], is shown as dashed lines.

The parameters used to calculate the theoretical curves differ somewhat from their estimates. The Gaussian pore size parameter is 2 μm rather than 1 μm. Also, it was found that $\Delta\chi$ had to be increased from 17×10^{-6} to 75×10^{-6} in order to obtain a match with the experimental data. The value of ρ_2 was found to be 16×10^{-6} m s^{-1}. The difference between 1 and 2 μm in a mercury injection determination of pore size is insignificant. It is likely that the discrepancy between the measured and fitted values of $\Delta\chi$ results from the crudeness of our model for the magnetic field gradient in the pore space of the rock; we consider this to be the most serious deficiency of the theory. The value of ρ_2 obtained is comparable to the value of ρ_1 deduced by Kenyon *et al.* (*26*) at an operating frequency of 10 MHz.

ACKNOWLEDGMENTS

We acknowledge enlightening discussions with C. Straley, E. J. Fordham, Professor L. D. Hall, J. Howard, Y. Hsu, W. Kenyon, and A. Sezginer. In addition, C. Straley provided invaluable assistance in keeping the NMR spectrometer in working order, and J. Howard generously provided a large quantity of petrographic data on the samples. M. Horsfield also thanks the Science and Engineering Research Council of Great Britain and the Herchel Smith Endowment for additional financial support.

REFERENCES

1. J. KARGER, H. PFEIFER, AND W. HEINK, *in* "Advances in Magnetic Resonance" (J. S. Waugh, Ed.), Vol. 12, p. 1, Academic Press, New York, 1988.
2. M. H. COHEN AND K. S. MENDELSON, *J. Appl. Phys.* **53,** 1127 (1982).
3. A. H. THOMPSON, S. W. SINTON, S. L. HUFF, A. J. KATZ, R. A. RASHKE, AND G. A. GIST, *J. Appl. Phys.* **65,** 3259 (1989).
4. W. P. HALPERIN, F. D'ORAZIO, S. BHATTACHARJA, AND J. C. TARCZON, *in* "Molecular Dynamics in Restricted Geometries" (J. Klafter and J. M. Drake, Eds.), Wiley, New York, 1989.

5. W. A. EDELSTEIN, H. J. VINEGAR, P. N. TUTUNJIAN, P. B. ROEMER, AND O. M. MUELLER, "63rd Annual Technical Conference and Exhibition of the Society of Petroleum Engineers, Houston, Texas, October 2–5 1988."
6. W. E. KENYON, P. I. DAY, C. STRALEY, AND J. F. WILLEMSEN, SPE Formation Evaluation, p. 622, September 1988.
7. H. Y. CARR AND E. M. PURCELL, *Phys. Rev.* **94,** 630 (1954).
8. S. MEIBOOM AND D. GILL, *Rev. Sci. Instrum.* **29,** 688 (1958).
9. P. STILBS, *Prog. NMR Spectrosc.* **19,** 1 (1987).
10. K. J. PACKER AND C. REES, *J. Colloid Interface Sci.* **40,** 206 (1972).
11. D. E. WOESSNER, *J. Phys. Chem.* **67,** 1365 (1963).
12. L. E. DRAIN, *Proc. Phys. Soc.* **80,** 1380 (1962).
13. R. C. WAYNE AND R. M. COTTS, *Phys. Rev.* **151,** 264 (1966).
14. B. ROBERTSON, *Phys. Rev.* **151,** 273 (1966).
15. C. H. NEUMAN, *J. Chem. Phys.* **60,** 4508 (1974).
16. J. C. TARCZON AND W. P. HALPERIN, *Phys. Rev. B* **32,** 2798 (1985).
17. M. ABRAMOWITZ AND I. E. STEGUN, "Handbook of Mathematical Functions with Formulas, Graphs, and Mathematical Tables," Chap. 10, U.S. National Bureau of Standards, 1964.
18. J. A. STRATTON, "Electromagnetic Theory," Section 3.28, McGraw–Hill, New York, 1941.
19. J. A. GLASEL AND K. H. LEE, *J. Am. Chem. Soc.* **96,** 970 (1974).
20. S. MAJUMDAR AND J. C. GORE, *J. Magn. Reson.* **78,** 41 (1988).
21. K. R. BROWNSTEIN AND C. E. TARR, *Phys. Rev. A* **19,** 2446 (1979).
22. R. J. S. BROWN, *Nature (London)* **189,** 387 (1961).
23. "DCADRE," IMSL, Houston, Texas; C. DE BOOR, *in* "Mathematical Software" (J. R. Rice, Ed.), Academic Press, New York, 1971.
24. S. LOWELL AND J. E. SHIELDS, "Powder Surface Area and Porosimetry," Chapman and Hall, London, 1984.
25. J. H. SIMPSON AND H. Y. CARR, *Phys. Rev.* **111,** 1201 (1958).
26. W. E. KENYON, J. J. HOWARD, A. SEZGINER, C. STRALEY, A. MATTESON, K. HORKOWITZ, AND R. EHRLICH, "Pore Size Distribution and N.M.R. in Microporous Cherty Sandstones," Society of Professional Well Log Analysts, 30th Annual Symposium, 1989.